Article

Cell Reports

# DNA Hydroxymethylation Profiling Reveals that *WT1* Mutations Result in Loss of TET2 Function in Acute Myeloid Leukemia

## Graphical Abstract

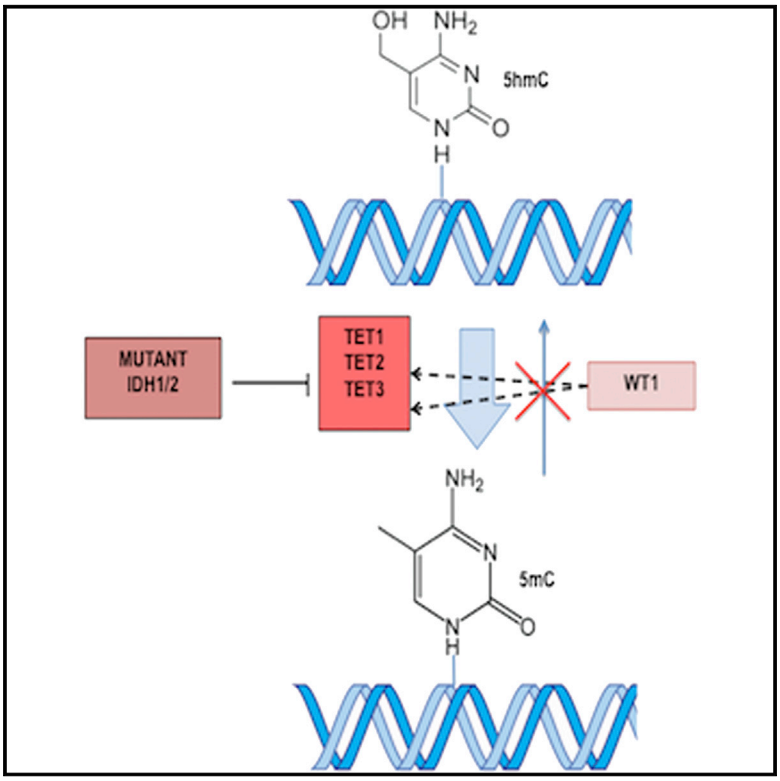


## Highlights

*WT1* mutations anticorrelate with *TET2* and *IDH1/IDH2* mutations in AML

*WT1* mutant AMLs have decreased global and locus-specific 5hmC levels

Changes in *Wt1* expression levels result in changes in 5hmC levels

WT1 binds TET2 and TET3, providing a link between WT1 and TET enzymatic function

## Authors

Raajit Rampal, Altuna Alkalin, ..., Maria E. Figueroa, Ross L. Levine

## Correspondence

chm2042@med.cornell.edu (C.E.M.), lgodley@medicine.bsd.uchicago.edu (L.A.G.), amm2014@med.cornell.edu (A.M.), marfigue@med.umich.edu (M.E.F.), leviner@mskcc.org (R.L.L.)

## In Brief

Mutational studies in patients with acute myeloid leukemia (AML) have identified recurrent mutations in *TET2* and *IDH1/IDH2*, and these mutations result in a reduction in 5-hydroxymethylcytosine (5hmC) levels. Rampal et al. demonstrate that *WT1* mutations anticorrelate with *TET2* and *IDH1/IDH2* mutations, and *WT1* mutant AMLs have decreased 5hmC levels, consistent with reduced TET2 function.

## Accession Numbers

GSE52945
GSE37454

Rampal et al., 2014, Cell Reports 9, 1841–1855
December 11, 2014 ©2014 The Authors
http://dx.doi.org/10.1016/j.celrep.2014.11.004

Cell Reports
Article



# DNA Hydroxymethylation Profiling Reveals that *WT1* Mutations Result in Loss of TET2 Function in Acute Myeloid Leukemia

Raajit Rampal,[1,2,22] Altuna Alkalin,[16,19,22] Jozef Madzo,[3,22] Aparna Vasanthakumar,[3,22] Elodie Pronier,[1] Jay Patel,[1] Yushan Li,[4] Jihae Ahn,[1] Omar Abdel-Wahab,[1,2] Alan Shih,[1,2] Chao Lu,[5] Patrick S. Ward,[5] Jennifer J. Tsai,[14] Todd Hricik,[1] Valeria Tosello,[6] Jacob E. Tallman,[1] Xinyang Zhao,[7] Danette Daniels,[17] Qing Dai,[8] Luisa Ciminio,[9] Iannis Aifantis,[9] Chuan He,[8] Francois Fuks,[15] Martin S. Tallman,[2] Adolfo Ferrando,[6] Stephen Nimer,[11] Elisabeth Paietta,[10] Craig B. Thompson,[5] Jonathan D. Licht,[12] Christopher E. Mason,[16,20,21,*] Lucy A. Godley,[3,13,*] Ari Melnick,[4,*] Maria E. Figueroa,[4,18,*] and Ross L. Levine[1,2,*]

[1]Human Oncology and Pathogenesis Program, Memorial Sloan-Kettering Cancer Center, New York, NY 10065, USA
[2]Leukemia Service, Department of Medicine, Memorial Sloan-Kettering Cancer Center, New York, NY 10065, USA
[3]Section of Hematology/Oncology, Department of Medicine, The University of Chicago, Chicago, IL 60637, USA
[4]Department of Hematology/Oncology, Weill Cornell Medical College, New York, NY 10065, USA
[5]Cancer Biology and Genetics Program, Memorial Sloan-Kettering Cancer Center, New York, NY 10065, USA
[6]Institute for Cancer Genetics, Columbia University Medical Center, New York, NY 10032, USA
[7]Molecular Pharmacology and Chemistry Program, Memorial Sloan-Kettering Cancer Center, New York, NY 10065, USA
[8]Department of Chemistry and Institute for Biophysical Dynamics, The University of Chicago, Chicago, IL 60637, USA
[9]Department of Pathology, New York University Cancer Institute, New York, NY 10016, USA
[10]Montefiore Medical Center, New York, NY 10466, USA
[11]Department of Medicine, Sylvester Comprehensive Cancer Center, Miami, FL 33136, USA
[12]Robert H. Lurie Comprehensive Cancer Center, Northwestern University, Chicago, IL 60611, USA
[13]The University of Chicago Comprehensive Cancer Research Center, Chicago, IL 60637, USA
[14]Department of Immunology and Microbial Pathogenesis, Weill Cornell Graduate School of Medical Sciences, New York, NY 10065, USA
[15]Laboratory of Cancer Epigenetics, Faculty of Medicine, Université Libre de Bruxelles, 1070 Brussels, Belgium
[16]Department of Physiology and Biophysics, Weill Cornell Medical College, New York, NY 10065, USA
[17]Promega Corporation, Madison, WI 53703, USA
[18]Department of Pathology, University of Michigan, Ann Arbor, MI 48109, USA
[19]Berlin Institute for Medical Systems Biology, Max Delbrück Centre for Molecular Medicine, Robert-Rössle-Straße 10, 13125 Berlin, Germany
[20]The HRH Prince Alwaleed Bin Talal Bin Abdulaziz Alsaud Institute for Computational Biomedicine, Weill Cornell Graduate School of Medical Sciences, New York, NY 10065, USA
[21]The Feil Family Brain and Mind Research Institute, Weill Cornell Graduate School of Medical Sciences, New York, NY 10065, USA
[22]Co-first author
*Correspondence: chm2042@med.cornell.edu (C.E.M.), lgodley@medicine.bsd.uchicago.edu (L.A.G.), amm2014@med.cornell.edu (A.M.), marfigue@med.umich.edu (M.E.F.), leviner@mskcc.org (R.L.L.)
http://dx.doi.org/10.1016/j.celrep.2014.11.004


## SUMMARY

Somatic mutations in *IDH1*/*IDH2* and *TET2* result in impaired TET2-mediated conversion of 5-methylcytosine (5mC) to 5-hydroxymethylcytosine (5hmC). The observation that *WT1* inactivating mutations anticorrelate with *TET2*/*IDH1*/*IDH2* mutations in acute myeloid leukemia (AML) led us to hypothesize that WT1 mutations may impact TET2 function. *WT1* mutant AML patients have reduced 5hmC levels similar to *TET2*/*IDH1*/*IDH2* mutant AML. These mutations are characterized by convergent, site-specific alterations in DNA hydroxymethylation, which drive differential gene expression more than alterations in DNA promoter methylation. WT1 overexpression increases global levels of 5hmC, and WT1 silencing reduced 5hmC levels. WT1 physically interacts with TET2 and TET3, and WT1 loss of function results in a similar hematopoietic differentiation phenotype as observed with TET2 deficiency. These data provide a role for WT1 in regulating DNA hydroxymethylation and suggest that *TET2 IDH1*/*IDH2* and *WT1* mutations define an AML subtype defined by dysregulated DNA hydroxymethylation.

## INTRODUCTION

Gene discovery studies in human cancers have identified novel mutations that inform new mechanisms of malignant transformation. Recurrent somatic mutations in epigenetic regulators compose an emerging class of disease alleles. Mutations in epigenetic modifiers have been observed in the majority of patients

with acute myeloid leukemia (AML), including mutations in DNA methyltransferases (Ley et al., 2010; Yan et al., 2011), chromatin modifying enzymes (Ernst et al., 2010), and histone methyltransferase readers (Wang et al., 2009). Notably, mutations in epigenetic modifiers and epigenetic signatures have been found to have prognostic and biologic relevance in AML (Bullinger et al., 2010; Figueroa et al., 2010b; Patel et al., 2012) and have led to the development of epigenetic therapies, in the context of clinical trials, for molecularly defined AML subsets (Bernt et al., 2011; Daigle et al., 2011; Dawson et al., 2011; Filippakopoulos et al., 2010; Zuber et al., 2011).

One class of mutations found in AML and in other malignancies affects the conversion of 5-methylcytosine (5mC) to 5hydroxymethylcytosine (5hmC), mediated by the TET family of enzymes. These include mutations in *TET2* and *IDH1*/*IDH2*. Mutational profiling of 398 patients with de novo AML demonstrated that *TET2* and *IDH1*/*IDH2* mutations were mutually exclusive and featured extensive promoter hypermethylation (Figueroa et al., 2010a; Patel et al., 2012). TET2 has been implicated in mediating demethylation of DNA with hydroxymethylation as an intermediate step in this process. TET2 loss of function results in reduction of genomic 5hmC and a reciprocal increase in 5mC (Ko et al., 2010). A similar effect is caused by aberrant production of the oncometabolite 2-hydroxyglutarate (2-HG) by gain-of-function *IDH1*/*IDH2* mutations, which result in inhibition of TET enzyme catalytic functions (Figueroa et al., 2010a). Hence, these mutations define a class of AMLs with reduced genome-wide 5hmC. Notably, mutations or altered expression of *IDH1*/*IDH2* and *TET* genes likewise result in altered 5hmC content in glioblastomas and melanomas (Lian et al., 2012). Yet, it has been shown that not all AML cases with low levels of 5hmC harbor somatic mutations in *TET2* and *IDH1*/*IDH2* (Konstandin et al., 2011). Hence, there are likely additional somatic mutations that can lead to direct or indirect alterations in TET enzyme function.

Recent technologic developments have enabled 5hmC mapping to be performed in normal tissues and in embryonic stem cells. These studies showed that 5hmC is commonly localized to gene regulatory elements, including promoters, gene bodies, and enhancers (Stroud et al., 2011). However, to date, genome-wide localization of 5hmC has not been reported in human malignancies, and the impact of *TET2* and *IDH1*/*IDH2* mutations and/or other mutations on 5hmC distribution has not been investigated. Cytosine methylation studies have often showed a weak inverse correlation between alterations in promoter DNA methylation and differential gene expression (Bell et al., 2011; Kulis et al., 2012), raising the possibility that other epigenetic modifications, such as 5hmC, may be more tightly linked with transcriptional changes.

In this study, we examined the mutational status, gene expression profiles, and cytosine methylation profiles of a cohort of 398 AML patients for novel mutations that might functionally overlap with *IDH1*/*IDH2* and *TET2*. Here, we show that *WT1* mutations are significantly reduced in frequency in patients with *TET2*/*IDH1*/*IDH2* mutant AML, and that *WT1* mutant AML is characterized by altered DNA methylation and global reductions in 5hmC similar to that observed in *TET2*/*IDH1*/*IDH2* mutant AML. Furthermore, we demonstrate that alterations in WT1 levels directly regulate 5hmC levels, which is due to an interaction between TET2/TET3 and WT1.

## RESULTS

### *WT1* Mutations Are Inversely Correlated with *IDH/TET2* Mutations in AML and Display Overlapping Promoter Hypermethylation Signatures

We recently performed mutational profiling of 398 AML patients and noted that *TET2* and *IDH1*/*IDH2* mutations were mutually exclusive (Figueroa et al., 2010a; Patel et al., 2012). We next investigated the same patient cohort for other mutations inversely correlated with *TET2* and *IDH1*/*IDH2* mutations. Mutations in the *WT1* gene were mutually exclusive of *IDH1*/*IDH2* mutations (Patel et al., 2012) and negatively correlated with *TET2* mutations (Figure 1A; Figure S1A). Twenty-eight of 313 (9%) of *TET2*/*IDH*-wild-type patients had somatic *WT1* mutations, whereas two of 85 (2%) *TET2*/*IDH1*/*IDH2* mutant patients had co-occurring *WT1* mutations ($p = 0.026$, Fisher's exact test, Table S1). We observed a similar inverse relationship between *WT1* mutations and *TET*/*IDH1*/*IDH2* mutations in the AML samples analyzed by TCGA (Table S2). Analysis of combined data from the ECOG1900 study and the AML TCGA data set confirmed a significant anticorrelation between *WT1* mutations and *TET2*/*IDH1*/*IDH2* mutations ($p = 0.0164$, Fisher's exact test, Table S3; Figure S1B). These data suggested a shared functional role for *WT1*, *TET2*, and *IDH1*/*IDH2* mutations in AML.

Using promoter DNA methylation microarrays (Figueroa et al., 2010a), we analyzed the DNA methylation profiles of 30 *WT1* mutant AML samples compared to 11 normal $CD34^+$ bone marrow cells and identified 653 differentially methylated regions (DMRs, see Experimental Procedures) in *WT1* mutant AML patients. The vast majority of the DMRs were aberrantly hypermethylated (Figure 1B). Next, we compared *WT1* mutant AML samples to a cohort of 29 AML1-ETO AMLs wild-type for *WT1*/*TET2*/*IDH1*/*IDH2* mutations and identified 124 DMRs, 68% ($n = 84$) of which were hypermethylated in *WT1* mutant AML patients (Figure 1C). *TET2* mutant and *IDH1*/*IDH2* mutant AML patients were also characterized by hypermethylation compared to *AML1-ETO*-positive AML (Figures S1C and S1D). Comparative analysis of the three hypermethylation profiles revealed a near-complete overlap of *TET2* and *WT1* hypermethylated loci within the *IDH1*/*IDH2* hypermethylation signature, and a highly significant overlap between the *TET2* and *WT1* mutant signatures (Fisher's exact test, p value $< 0.001$ for all comparisons) (Figure 1D), consistent with convergent, site-specific effects on DNA methylation.

### *WT1*, *TET2*, and *IDH1/IDH2* Mutations Are Characterized by Global Reductions in 5hmC in Primary AML Samples

Given that *IDH1*/*IDH2* mutations or silencing of *TET2* leads to reduced 5hmC levels in hematopoietic cells (Figueroa et al., 2010a; Ko et al., 2010), we hypothesized that AML patients with *WT1* mutations would also be characterized by reduced 5hmC due to reduced TET enzymatic function. Liquid chromatography-electron spray ionization-tandem mass spectrometry (LC-ESI-MS/MS) revealed that *WT1* mutant AML patients had significantly reduced 5hmC when compared to AML patients

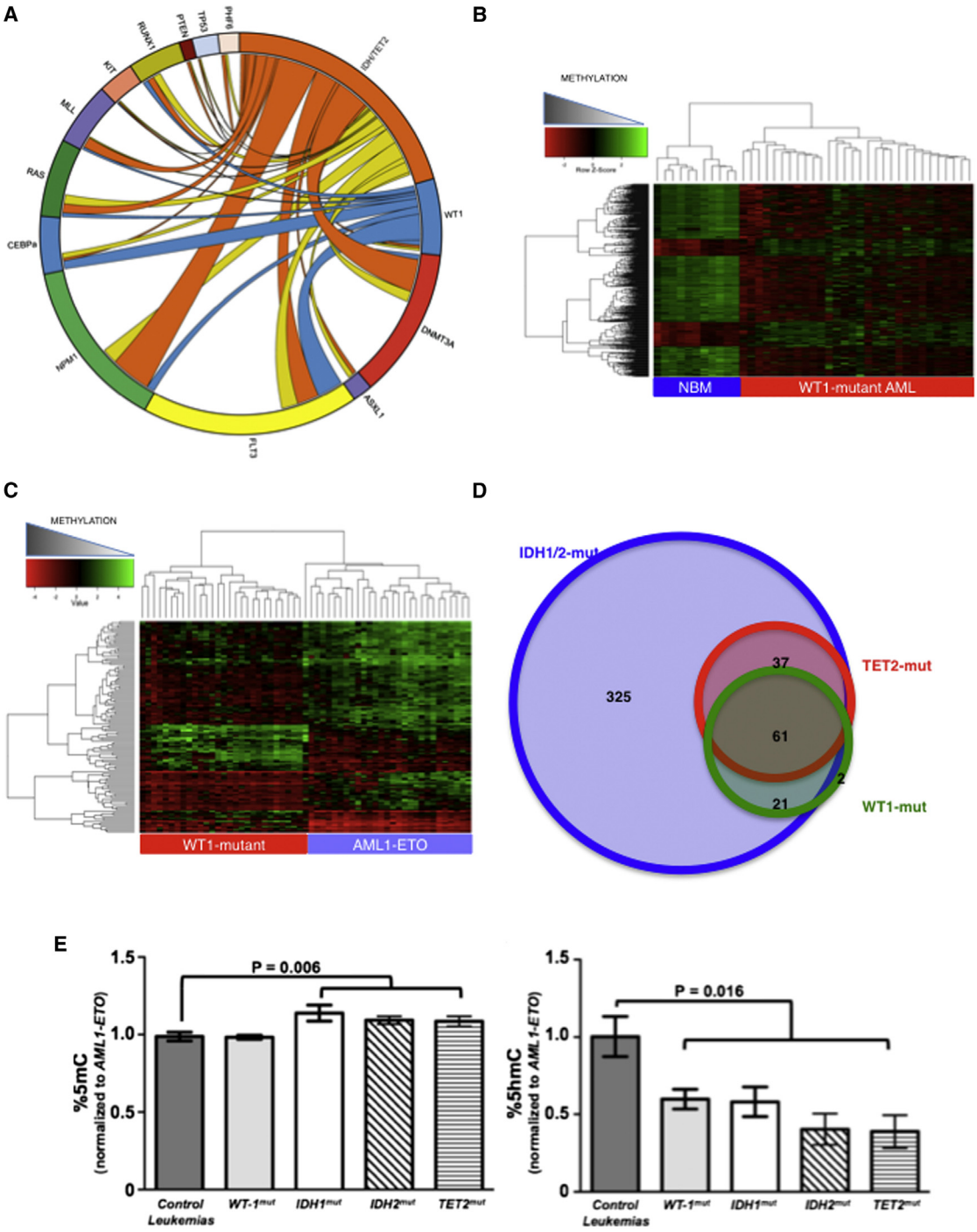


**Figure 1. *WT1* Mutations Are Inversely Correlated with *TET2*/*IDH1*/*IDH2* Mutations and Display Similar Global Methylation Profile**

(A) Circos representation of targeted mutational data from 398 AML patients. Co-occurrence of mutations is represented by lines connecting genes. The width of connecting lines represents frequency of mutations. *TET2* and *IDH* mutations are combined in this analysis. *IDH* mutations are designated by orange ribbons, *TET2* mutations by yellow ribbons, and *WT1* mutations by blue ribbons.

(B) Promoter methylation signatures in *WT1* mutant AML versus normal bone marrow (NBM).

(C) Comparison of promoter methylation signatures in *WT1* mutant AML and AML1-ETO AML.

(D) Overlap of hypermethylated loci in *WT1* mutant AML compared with those previously identified in *TET2* and *IDH1*/*IDH2* mutant AMLs.

(E) 5-methylcytosine (5mC, left) and 5-hydroxymethylcytosine (5hmC, right) levels in AML samples from patients with or without *WT1*, *TET2*, or *IDH1*/*IDH2* mutations. 5mC and 5hmC levels were determined by liquid chromatography-electron spray ionization-tandem mass spectrometry (LC-ESI-MS/MS). Error bars represent SEM.

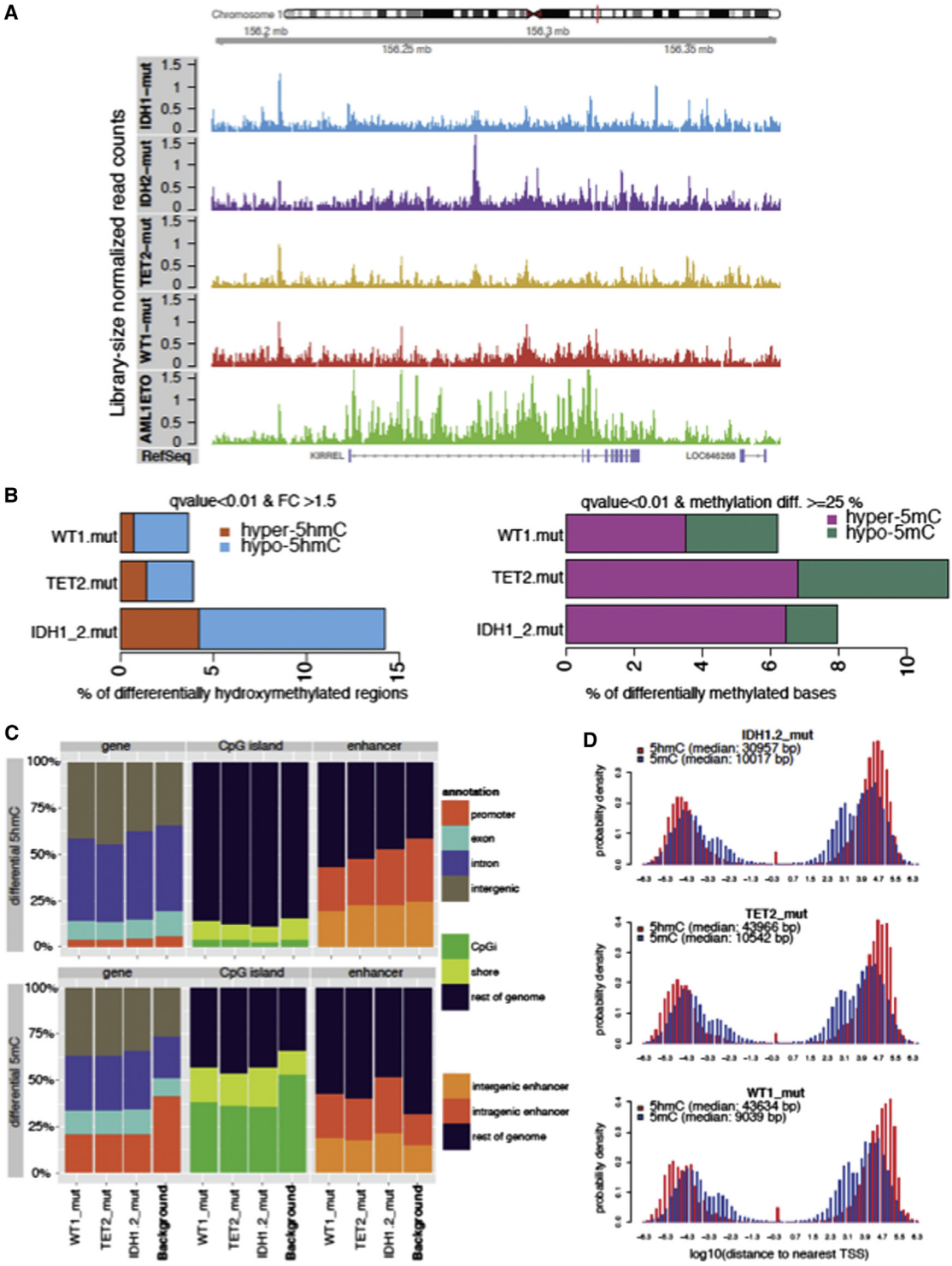


**Figure 2. Convergent, Site-Specific Alterations in DNA Hydroxymethylation in AML Patients with *TET2*, *IDH1*/*IDH2*, and *WT1* Mutations**

(A) KIRREL locus demonstrating depletion of 5hmC marks in AML patients with *TET2*, *WT1*, and *IDH1*/*IDH2* mutations.

(B) Percentages of differential 5hmC regions and 5mC bases. Bar plot on the left demonstrates percentages of hypo- or hyper-5hmC regions out of all canonical peaks in *WT1*, *TET2*, and *IDH1*/*IDH2* mutants compared to AML1-ETO patients. Bar plot on the right demonstrates the percentages of hypo- and hyper-methylated CpGs out of all covered CpGs in *WT1*, *TET2*, and *IDH1*/*IDH2* mutants compared to AML1-ETO patients. Differentially methylated CpGs that overlap with differential 5hmC regions are removed from the analysis.

*(legend continued on next page)*

wild-type for *WT1*, *TET2*, or *IDH1/IDH2* (p = 0.016 t test, Figure 1E). Similarly, the reduction in 5hmC levels was comparable in extent in *WT1* mutant AML patients compared to *IDH1/IDH2* mutant and *TET2* mutant AML patient samples. This finding was confirmed by dot-blot analysis (Song et al., 2011) (Figure S1E). Although global cytosine methylation abundance was significantly increased in *IDH1*, *IDH2*, and *TET2* mutant patients, there was no significant increase of 5mC in *WT1* mutant AML, suggesting that *WT1* mutant AML is primarily characterized by alterations in 5hmC leading to site-specific effects on DNA methylation rather than a global increase in 5mC.

### 5hmC Mapping Reveals Similar Alterations in 5hmC Localization in *WT1*, *TET2*, and *IDH1/IDH2* Mutant AML

In order to determine the impact of *IDH1/IDH2*, *WT1*, and *TET2* mutations on the distribution of epigenetic marks throughout the genome more precisely, we examined 5mC and 5hmC localization in primary AML specimens with next-generation sequencing. Once again, specimens with *AML1-ETO* translocation, which are all wild-type for *IDH1/IDH2*, *TET2*, and *WT1*, were profiled as a control AML cohort. We used a selective chemical labeling approach followed by streptavidin capture and sequencing to map the abundance and distribution of 5hmC (hMe-Seal, see Experimental Procedures) (Song et al., 2011). We identified areas of 5hmC enrichment for each sample with ChIPseeqer (Giannopoulou and Elemento, 2011). The average number of peaks identified in AML1-ETO specimens was 192,066, for *TET2*-mut 114,865, for *IDH1/IDH2* 70,622, and for *WT1-mut* 60,258. The average number of 5hmC peaks called per sample was significantly lower in AML patients with *TET2*, *WT1*, *IDH1*, or *IDH2* mutations compared to control AMLs (t test p values between 0.0005 and 0.003 for all comparisons; see Figure 2A as an example for regions of loss of 5hmC and Figure S2A for overall changes in 5hmC loss). These data are consistent with the global reduction in 5hmC observed by mass spectrometry (Figure 1E). We calculated pairwise comparisons of peaks of 5hmC enrichment in *IDH1/IDH2*, *WT1*, and *TET2* mutant AML against 5hmC sites identified in control AML patients. All three AML subtypes (*IDH1/IDH2*, *WT1*, and *TET2*) displayed a significant reduction in 5hmC peaks across the entire genome versus controls, with a smaller proportion (between 1% and 5%) of regions presenting with gains in 5hmC (Figure 2B). We then performed DNA methylation bisulfite sequencing by enhanced reduced representation bisulfite sequencing (ERRBS) on the same patients to map the distribution of 5mC. ERRBS assayed 1,433,193 CpGs across all AML subtypes. Pairwise differential methylation comparisons performed on these ERRBS profiles revealed that 5mC levels increased genome-wide in *IDH1/IDH2*, *WT1*, and *TET2* compared to control AML patients; specifically, 4%–6.5% of CpGs were methylated, in *IDH1/IDH2*, *TET2*, and *WT1* mutations (see Figure 2B). This contrasts with the reduced levels of 5hmC in these samples. These observations, specifically the loss of 5hmC and gain of 5mC in WT1 mutant, TET2 mutant, and IDH1/IDH2 mutant AML patients, also hold when we compared 5hmC and 5mC levels against normal bone marrows (NBMs; see Figure S2). Moreover, AML1-ETO AMLs showed no significant difference in the average total number of 5hmC peaks when compared to NBMs, indicating that the reduction of 5hmC peaks is specific to those AMLs with disruption of *TET2*, *IDH1/IDH2*, or *WT1* (Figure S2B).

### Aberrant 5hmC Distribution in *WT1*, *TET2*, and *IDH1/IDH2* Mutant AML Occurs Predominantly at Enhancers and Distal Regulatory Elements

Next, we sought to determine whether *IDH1/IDH2*, *WT1*, and *TET2* somatic mutations affect not only the abundance but also the genomic distribution pattern of 5hmC. We first examined 5hmC peak profiles in patient specimens through unsupervised analyses using hierarchical clustering and multidimensional scaling (MDS), which can be thought of as 2D representations of pairwise distance between samples. Hierarchical clustering and MDS results show the relationship between different samples based on their 5hmC and 5mC profile similarities. *IDH1* and *IDH2* mutant AMLs exhibited the most significant difference in 5hmC and clustered furthest away from the control AMLs (Figures S2C and S2D). *WT1* and *TET2* mutant AML patients clustered closer to each other and localized in between *IDH1/IDH2* and control AML patients in the first dimension of the multidimensional scaling. These findings suggest the underlying alterations in 5hmC patterning in *TET2* and *WT1* mutant AMLs are less widespread across the genome than in AML specimens carrying *IDH1/IDH2* mutations. Given that 2-HG is predicted to inhibit the function of all three TET enzymes (Xu et al., 2011), these data are consistent with more profound pan-TET enzyme inhibition in *IDH1/IDH2* mutant AML. Regardless of AML subtype, 5hmC peaks were most commonly (52%–59%) located within gene bodies and somewhat less commonly in intergenic regions (37%–44.2% across subtypes). Less than 5% of 5hmC peaks were found at promoter regions (Figure 2C). Most regions with differential 5hmC enrichment in *IDH1/IDH2*, *WT1*, and *TET2* AMLs were located at a significant distance from transcription start sites (median distance between 31 and 44 kb). By contrast, differentially methylated loci were closer to the TSS of known genes, suggesting that the perturbation of 5hmC and 5mC patterns in *IDH1/IDH2*, *WT1*, and *TET2* AMLs can occur at distinct genomic regions (Figure 2D). Most regions with differential 5hmC enrichment were located outside of CpG islands and CpG island shores (87%–89%). Yet, about half of the differential 5hmC peaks were located at enhancer regions as defined by the ENCODE project (see the Experimental Procedures) (43%–53%) (Figures 2C and 2D), suggesting differential 5hmC localization at enhancers may contribute to aberrant gene expression in leukemia.

(C) Genomic locations of differentially hydroxymethylated regions (DHMRs) and differentially methylated cytosines (DMCs). The first row shows percentages of DHMRs overlapping with gene annotation, CpG island annotation, and enhancer annotation. The second row shows the percentage of DMCs overlapping with the aforementioned annotation categories.

(D) Distances to nearest TSS for DHMRs and DMCs for *IDH1/IDH2*, *TET2*, and *WT1* mutants. All comparisons are against AML1-ETO patients.

### Differential 5hmC More Strongly Correlates with Differential Gene Expression than Differential 5mC in AML with *WT1*, *TET2*, and *IDH1/IDH2* Mutations

The distinct localization patterns of 5mC and 5hmC raised the question of whether these marks can function independently to coordinate gene expression. We used gene expression profiling to compare *TET2-mut*, *IDH1/IDH2-mut*, and *WT1-mut* against AML-1ETO and identify the top 500 upregulated and the top 500 downregulated genes in the same AML samples (see the Experimental Procedures for details). We then examined the relationship between changes in gene expression with changes in 5mC and 5hmC abundance in each leukemia subtype (*IDH1*, *IDH2*, *TET2*, and *WT1*). As expected, differential cytosine methylation at promoters was negatively correlated with gene expression (Figure 3A, top) but with a relatively low correlation coefficient ($r = -0.348$ to $-0.4$, Pearson's R test p values between 0.02 and 0001 in the different AML subsets). By contrast, 5hmC changes in gene body and distal regulatory regions had a positive correlation with gene expression and showed a much stronger and more significant correlation ($r = 0.52$-$0.75$, Pearson's R test p value between $10^{-9}$ and $10^{-14}$) in the different AML subsets (Figure 3A, bottom) than the correlation observed with 5mC levels. 5hmC changes were strongly correlated with differential expression regardless of genomic location, including first introns ($r = 0.75$, Pearson's R test p values $< 0.0001$), distal regions ($r = 0.69$, Pearson's R test p value $< 0.0001$), gene bodies ($r = 0.67$, Pearson's R test p values $< 0.0001$), and promoter region ($r = 0.61$, Pearson's R test p values $< 0.0001$) (Figure S3A). By contrast, 5mC changes were most strongly correlated with gene expression when present near TSS and on first intron but less strongly correlated with gene expression when present at other genomic locations investigated (CpG island shores and gene body; Figure S3B).

Next, we sought to determine which of these two epigenetic marks could more accurately predict changes in gene expression. We used a machine-learning model for predicting differentially expressed genes using differential methylation and hydroxymethylation. In *IDH1/IDH2* mutant and *TET2* mutant AML, 5hmC levels at enhancers performed better than 5mC present at promoters at predicting gene expression, judging from AUC (area under receiver operator curves). The AUC shows the performance of the classifier where AUC of 1 will indicate a perfect model, whereas a random model will have an AUC of 0.5 (Figure 3B). For each model, we measured the AUC using 10-fold cross-validation, which gives a distribution of AUC values for each model that is generated by training and testing models with randomized subsets of the whole data set. In *WT1* mutant AML, differential 5mC and differential 5hmC occupancy independently predicted gene expression equally well (similar AUC values), but a model with combined 5hmC and 5mC attributes increased classification performance judging by mean AUC values from cross-validation models (Figure 3B). When comparing the AUC from the different models, the performance of 5hmC + 5mC and 5hmC models were significantly better at predicting gene expression (pairwise t test p values between $10^{-9}$ and $10^{-8}$). Our findings are consistent with 5hmC functioning as an independent epigenetic mark that is linked to potential distal regulation, and suggests that 5hmC has additional functions independent of its role of an intermediate step to DNA demethylation at gene promoters (Yu et al., 2012).

### Site-Specific 5hmC Alterations in *TET2/WT1* Mutant AMLs Compose a Subset of the Alterations Seen in *IDH1/IDH2* Mutant AML

The data presented above suggest a potential unifying link between *IDH1/IDH2*, *TET2*, and *WT1* mutant AMLs. We therefore assessed site-specific alterations in 5hmC in *IDH1/IDH2*, *TET2*, and *WT1* mutant AMLs. *IDH1/IDH2* mutant AMLs displayed the greatest number of hydroxymethylation peaks lost ($n = 20{,}286$) compared to control AML specimens (AML1-ETO AMLs). By contrast, *TET2* mutant and *WT1* mutant AML samples had fewer 5hmC peaks lost ($n = 5{,}030$ and $5{,}484$, respectively). However, 68% of the peaks lost in *WT1* mutant specimens and 81% of those lost in *TET2* mutant AML overlapped with those lost in *IDH1/IDH2* mutant AML (Figures 4A and 4B; Figure S3C). We observed highly significant overlap of differential 5hmC peaks lost in *WT1* mutant AML and *TET2* mutant AML (Figure 4B) (hypergeometric test p value $<10^{-133}$). In a manner analogous to the findings for 5hmC, the hypermethylated sites identified in *WT1/TET2* mutant AML were a subset of those found in *IDH1/IDH2* mutant cases (Figures 4C and 4D). 44% of peaks of promoter hypermethylation identified in *TET2* mutant AML and 65% of those of *WT1* mutant specimens overlap with peaks of 5mC in *IDH1/IDH2* mutant AML (hypergeometric test p value $<10^{-133}$). Collectively these data suggest that a core set of deregulated and presumably silenced genes might represent a unifying pathway in *IDH1/IDH2*, *TET2*, and *WT1* mutant AML.

Although WT1 is a sequence-specific transcription factor, the mechanisms by which TET2 is recruited to specific loci to convert 5mC to 5hmC have not been delineated. To define candidate transcription factors (TFs) that might be important for TET2 action, we examined regions of differential 5hmC modification for the presence of specific DNA motifs characteristic of known TFs. This motif analysis revealed an overrepresentation of ETS motifs with GGAA core sequence (Figures S4A and S4B) in regions with 5hmC enrichment. Notably, we observed that regions with loss of 5hmC peaks in WT1 mutant AML cases were enriched for a AGG[AC]AGG (CCT[TG]CCT) motif that is analogous to a WT1 binding motif reported by Wang et al. (1993). Consistent with these data, we observed colocalization of WT1 and TET2 at specific loci with 5hmC enrichment, including *SHANK1* (Figure S4C). We also observed WT1 occupancy at regions with differential 5hmC, which are not bound by TET2, suggesting that other factors including other TET proteins might colocalize with WT1 at other gene regulatory elements (Figure S4D). We also curated chromatin immunoprecipitation sequencing experiments to identify myeloid lineage specific transcription factors that were enriched at regions with differential 5hmC in AML cells. This showed that ETS factors like FLI1, ERG, and their binding partners RUNX1 and CEBPA/B (Figure S4E) were enriched in regions of increased 5hmC, but not in hypo-5hmC regions, suggesting these transcription factors bind to regions with increased 5hmC, but are not enriched at sites with reduced 5hmC in *IDH1/IDH2*, *TET2*, and *WT1* mutant AML.

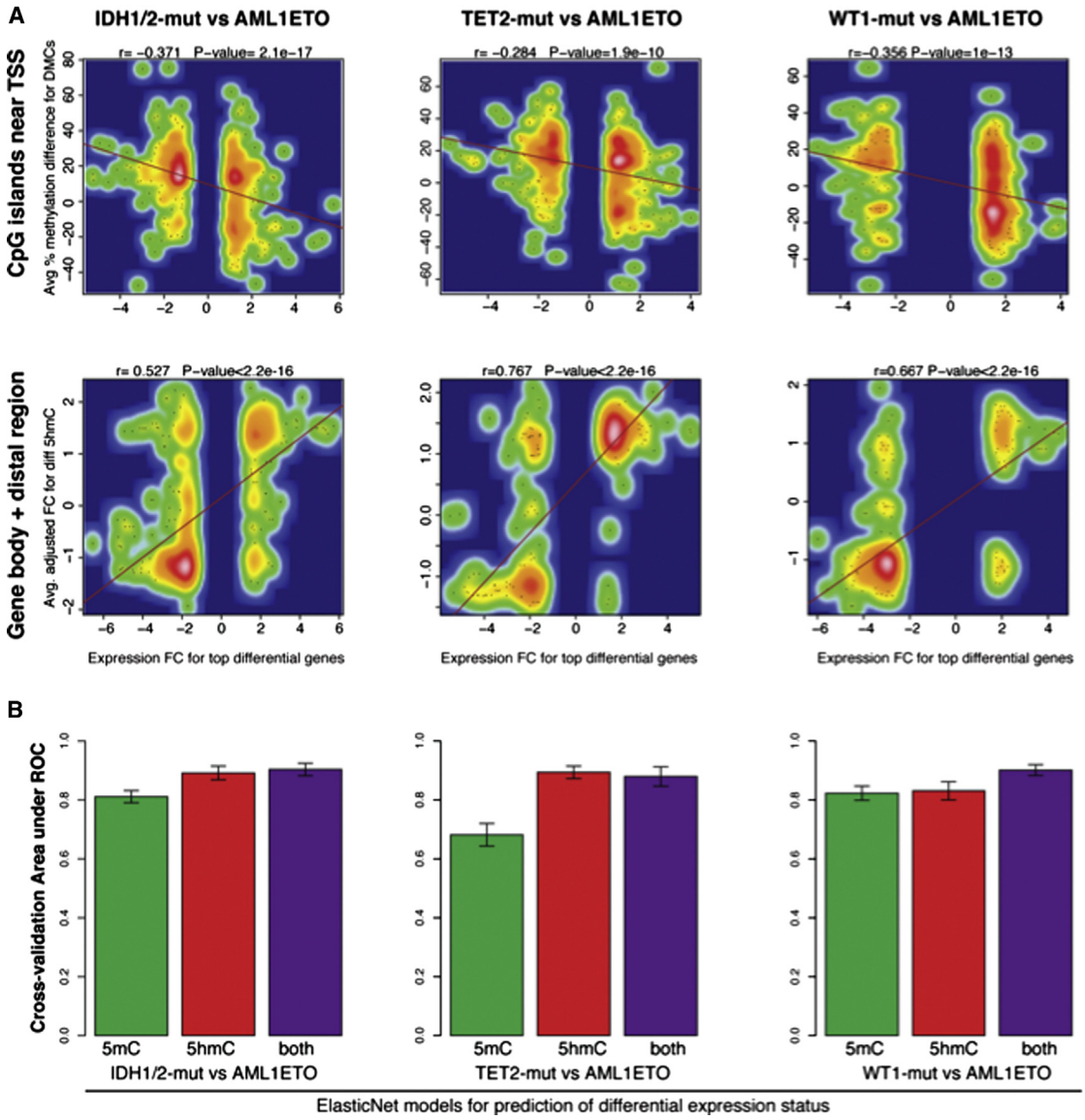


**Figure 3. Correlation of Gene Expression with DNA Methylation and Hydroxymethylation**

(A) Scatterplots and correlations of differential gene expression and average methylation difference on CpG islands near TSS for IDH-mut versus AML1-ETO, TET2-mut versus AML1-ETO, and WT1-mut versus AML1-ETO (top row). Scatterplots and correlations of differential gene expression and average adjusted fold changes of 5hmC canonical peaks for IDH-mut versus AML1-ETO, TET2-mut versus AML1-ETO, and WT1-mut versus AML1-ETO (bottom row).

(B) Mean AUC (area under receiver operator curve) for gene expression classification models based on differential 5mC and 5hmC attributes for IDH-mut versus AML1-ETO, TET2-mut versus AML1-ETO, and WT1-mut versus AML1-ETO. Classification models are based on differential 5hmC attributes and/or differential 5mC attributes aiming to predict upregulated and downregulated genes. Error bars represent SD of AUC of the cross-validation models.

## WT1 Directly Regulates 5hmC Levels in Hematopoietic Cells

The overlap in regions of 5hmC lost when *TET2* and *WT1* were mutated in AML and the inverse association between *WT1* and *TET2* mutations in AML suggested a potential functional interaction between these two proteins, and that WT1 might play a direct role in regulating TET-mediated hydroxymethylation. Previous studies have shown that AML-associated *WT1* mutations result in premature stop codons or are targeted by nonsense-mediated decay (Abbas et al., 2010), which results in loss of WT1 protein expression. We therefore investigated the effects of WT1 loss of function on 5hmC levels in M15 murine mesonephron cells, which express high levels of *Wt1* (Larsson et al., 1995). Knockdown of *Wt1* in M15 cells significantly decreased 5hmC levels in M15 cells ($p < 0.01$, t test) (Figures 5A and 5B). Similarly, in primary murine bone marrow (BM) cells, silencing of *Wt1* by small hairpin RNA (shRNA) (Vicent et al., 2010) (Figures S5A and S5B) significantly reduced 5hmC compared to cells expressing an empty vector (Figure 5C) ($p < 0.01$, t test). Similar effects were observed in primary murine BM cells transduced with

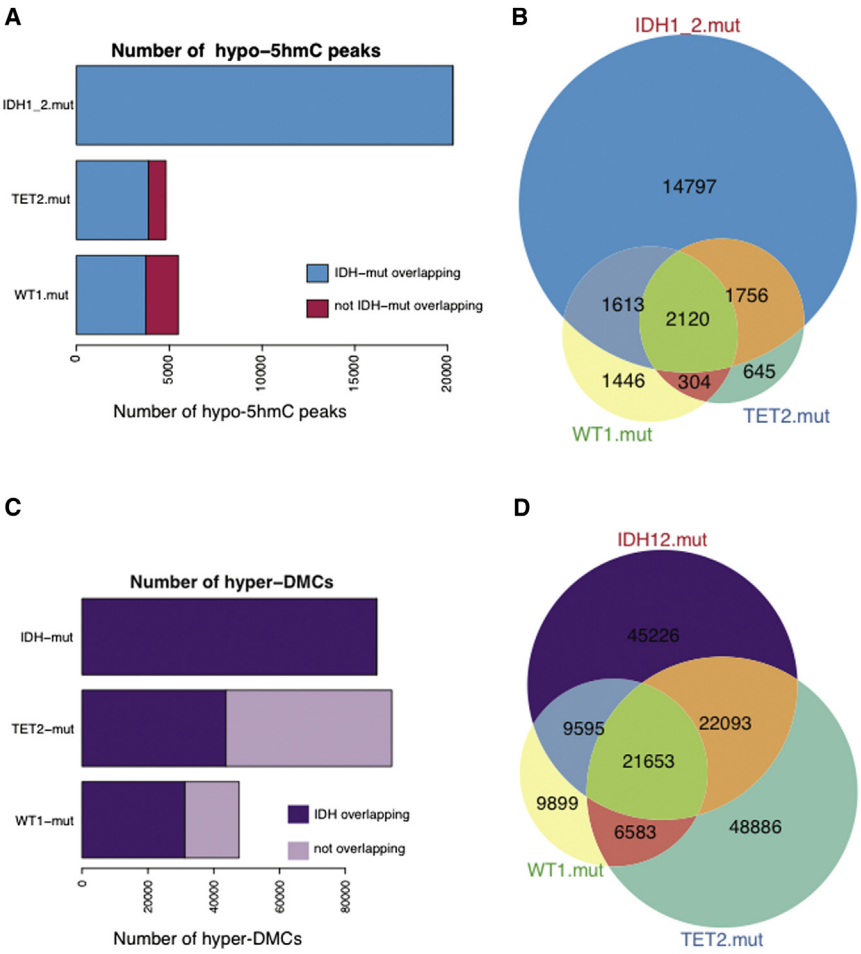


**Figure 4. Site-Specific 5-Hydroxymethylcytosine Alterations in *WT1* and *TET2* Mutant AML Compose a Subset of the Alterations in *IDH1/IDH2* Mutant AML**

(A) Bar plots showing number of hypo-DHMRs per subtype compared to AML1-ETO. For each subtype, the number of hypo-DHMRs that do not overlap with hypo-DHMRs of IDH-mut is color coded.

(B) Venn diagram showing the number hypo-DHMRs for each subtype and their overlap.

(C) Bar plots showing number of hyper-DMCs per subtype compared to AML1-ETO. For each subtype, the number of hyper-DMCs that do not overlap with hyper-DMCs of IDH-mut is color coded.

(D) Venn diagram showing the number hyper-DMCs for each subtype and their overlap.

*Tet2* shRNA (Figure S5C). Perturbations in WT1 did not significantly alter proliferation (Figure S5D). These convergent data suggest that reductions of 5hmC levels in AML could be a direct result of loss of WT1 function in AML.

Previous studies have shown that overexpression of wild-type *WT1* can contribute to malignant transformation in AML (Nishida et al., 2006), lung cancer (Oji et al., 2002; Vicent et al., 2010), and in Wilms tumor cases without *WT1* mutations (Kim et al., 2008). We therefore evaluated whether *WT1* overexpression could lead to increases in 5hmC, and if AML-associated *WT1* mutations abrogated the ability of WT1 to impact 5hmC. The most commonly expressed *WT1* isoform (isoform D) contains exon 5 (17AA$^{+}$) and a KTS site between exons 3 and 4 (Haber et al., 1991), hereafter referred to as *WT1*$^{+/+}$. We first expressed wild-type WT1$^{+/+}$ and a *WT1*$^{+/+}$ construct with a known AML truncation mutant in exon 7 (*WT1* mutant) in 32D myeloid cells. WT1$^{+/+}$ expression significantly increased 5hmC levels compared to cells expressing a control vector or *WT1* mutant ($p < 0.05$ for either comparison) (Figure 5D). *WT1* overexpression did not alter the expression of TET1, TET2, or TET3 (Figure S5E). In addition, shRNA-mediated knockdown of *WT1* in primary human CD34$^{+}$ cells did not result in changes in *TET1*, *TET2*, or *TET3* expression levels, and WT1 silencing or WT1 overexpression in K562 did not alter TET2 protein expression (Figures S5F–S5H). Expression analysis of the ECOG1900 cohort data demonstrated *TET1*, *TET2*, and *TET3* mRNA were expressed at similar levels in *WT1* mutant AML patient samples compared to WT1 wild-type AML cases, and *WT1* expression was not altered in *TET2* mutant versus *TET2* wild-type cases, nor in *IDH1/IDH2* mutant versus *IDH1/IDH2* wild-type cases (Figures S6A–S6C). We observed no changes in WT1 expression in *TET2* mutant AML patients in the TCGA data set (data not shown). In contrast to mutant *IDH1/IDH2* alleles, expression of *WT1*$^{+/+}$ or *WT1* mutant proteins did not impact 2-HG levels in hematopoietic cells (Figure S6D). Taken together, these data suggest alterations in WT1 expression do not regulate DNA hydroxymethylation by altering TET enzyme expression or by altering IDH1/IDH2 enzymatic function.

## WT1 Forms a Complex with TET2 in Hematopoietic Cells

Given the effects of WT1 on 5hmC levels and the inverse correlation between WT1 and TET2 mutations in AML, we hypothesized that WT1 might modulate TET2 function through direct interaction. Coimmunoprecipitation experiments in 293T cells revealed that WT1 interacts with TET2 (Figure 5E; Figure S6E). This interaction was not abrogated by ethidium bromide exposure (Figure S6F), consistent with a DNA-binding-independent interaction. We next did coimmunoprecipitation studies to determine the domain(s) of WT1 that are required for interaction with TET2. The different isoforms of WT1 also interact with TET2, suggesting the KTS domain is dispensable for TET2 interaction (Figure S6F). Deletion of the zinc-finger domain abrogated binding of WT1 to TET2, whereas truncation of the N-terminal region did not alter TET2 binding (Figure 5F). We did not observe interaction of WT1 or TET2 with HDAC6, suggesting the interaction between WT1 and TET2 is not due to nonspecific association of highly expressed nuclear proteins (Figure S6G). Coimmunoprecipitation

studies revealed interaction of endogenous TET2 and WT1, in HEL and Nomo-1 cells, confirming endogenous WT1 and TET2 can directly interact in hematopoietic cells (Figure 6G). As a control, we did not observe any association between TET2 and WT1 in AML14 cells, which do not express detectable levels of TET2 protein (Figure 6G). Coimmunoprecipitation was also performed using buffer with increasing NaCl concentrations, which did not result in abrogation of the interaction between WT1 and TET2 (Figure S6H).

### WT1 Loss Leads to Impaired Hematopoietic Differentiation Similar to that Observed with TET2 Loss

We and others have showed that loss of *Tet2* expression leads to expansion of c-Kit positive cells in vitro and in vivo (Li et al., 2011; Moran-Crusio et al., 2011; Quivoron et al., 2011). *Wt1* silencing in primary hematopoietic cells using two independent hairpins led to a similar increase in c-kit expression (Figure 6A; Figure S7A) ($p < 0.05$ t test). Furthermore, *Wt1* silencing in primary murine BM cells led to expansion of the lineage-negative, Sca-positive, Kit-positive stem/progenitor population to a similar extent as observed with *Tet2* downregulation (Figure S7B). Previous studies have revealed a role for TET2 in myelomonocytic fate commitment (Ko et al., 2010). *Wt1* silencing led to an increase in the population of CFU-GEMM (colony forming unit-granulocyte, erythrocyte, macrophage, megakaryocyte) similar to that observed with *Tet2* silencing (Figure 6B). Given the observations that WT1 expression can modulate 5hmC levels, and that *Wt1* downregulation in hematopoietic cells can recapitulate phenotypes associated with *Tet2* downregulation, we examined the transcriptional profile of primary murine BM cells transduced with vector or hairpins targeting *Tet2* or *Wt1*. We found a significant overlap between differentially expressed genes in primary murine BM cells transduced with shRNA targeting *Tet2* or *Wt1*, when compared with vector-transduced cells (hypergeometric test $p < 10^{-50}$, Figure S7C; Table S4). Collectively, these data indicate that reduced *Wt1* expression has similar effects on hematopoietic differentiation as observed with *Tet2* attenuation.

### WT1 Expression Rescues the Effects of TET2 Loss through Interactions with TET3 In Vivo

We next determined whether overexpression of *WT1* could attenuate the effects of *Tet2* loss. Expression of $WT1^{+/+}$, but not a *WT1* mutation observed in AML patients, significantly reduced colony growth in *Tet2*-deficient cells at primary and secondary plating ($p < 0.01$, t test) (Figure 6C; Figure S7D). Mass spectrometric analysis revealed that expression of $WT1^{+/+}$, but not *WT1* mutant increased 5hmC levels in *Tet2* KO cells (Figure 6D). Accordingly, overexpression of wild-type, but not mutant, WT1 reduced c-Kit expression, consistent with restored hematopoietic differentiation (Figure 6E). In order to assess whether loss of *Wt1* produced an additive phenotype in conjunction with *Tet2* loss, shRNA targeting *Wt1* was transduced into *Tet2* KO cells and plated in methylcellulose. No increase in colony formation was noted with concomitant *Tet2*/*Wt1* loss (Figure S7E). By contrast, expression of wild-type WT1, but not mutant WT1, abrogated the ability of Tet2 knockout cells to reconstitute hematopoiesis in vivo (Figure 6F).

The observation that wild-type WT1, rescued 5hmC levels, and abrogated the phenotype of *TET2*-deficient cells suggested the possibility that WT1 might also regulate the activity of the other TET enzymes. Expression of $WT1^{+/+}$ in the presence of 1-octyl-D-2-hydroxyglutarate (octyl-2HG, a cell permeable form of 2-HG) (Lu et al., 2012), which inhibits the activity of all alpha-ketoglutarate-dependent TET enzymes, inhibited the ability of WT1 to alter 5hmC levels consistent with a TET-family-dependent effect of WT1 (Figure 7A). Consistent with these data, coimmunoprecipitation studies demonstrated WT1 directly interacts with TET3, but not TET1 (Figure 7B). We next sought to determine if TET3 could modulate WT1-mediated effects on hematopoiesis in the absence of TET2. We coexpressed WT1 with two different validated shRNA constructs against Tet3 in *Tet2*-deficient BM cells. When *Tet3* was silenced in $Tet2^{-/-}$ marrow, WT1 could no longer suppress hematopoietic colony formation, demonstrating that Tet3 can act as a WT1 effector in the absence of Tet2 (Figures 7C and S7F). These data indicate WT1 is able to interact with TET2 and TET3, and that WT1 overexpression can rescue the effects of TET2 loss in a TET3-dependent manner.

## DISCUSSION

Here, we report that *WT1* mutations are inversely correlated with *TET2* and *IDH1*/*IDH2* mutations in AML, and that *WT1* mutant AML samples are characterized by significantly marked reductions in global and site-specific DNA hydroxymethylation. We show that WT1 interacts with TET2 and TET3, and that alterations in *WT1* expression regulate 5hmC abundance. Our genetic, epigenetic, and biochemical data indicate that *TET2*, *IDH1*/*IDH2*, and *WT1* mutant AMLs are characterized by disordered DNA hydroxymethylation potentially representing a convergent mechanism of leukemic transformation involving disordered DNA hydroxymethylation. These data also suggest that, in addition to its role as a sequence-specific transcription factor, WT1 may act as a cofactor for TET enzymes recruiting or stimulating their activity at specific sites in the genome.

We also employed next-generation sequencing methodologies to map 5hmC localization in AML patients with and without *WT1*, *TET2*, and *IDH1*/*IDH2* mutations. We observed differential 5hmC localization at enhancers, gene bodies, and distal regulatory elements and differential 5mC localization at intronic regions near transcription start sites in *IDH1*/*IDH2*, *TET2*, and *WT1* mutant AMLs. Moreover, we observed a strong, positive correlation between 5hmC changes and gene expression as compared to a weaker inverse correlation with 5mC. These data suggest that 5hmC has distinct effects on gene regulation independent of its role as an intermediate step to DNA demethylation, and also indicate that 5hmC may regulate enhancers/chromatin conformation, histone state, and/or transcription factor binding. Subsequent studies using base-pair resolution mapping of 5hmC and other recently described DNA modifications, combined with mapping other *cis*/*trans*-acting elements will help elucidate the complex roles of 5hmC and other DNA modifications on gene regulation in different cellular contexts.

Our 5hmC profiling data in AML samples with *IDH1*/*IDH2*, *WT1*, and *TET2* mutations reveal site-specific loss of 5hmC in AMLs with impaired TET function, which is most widespread in

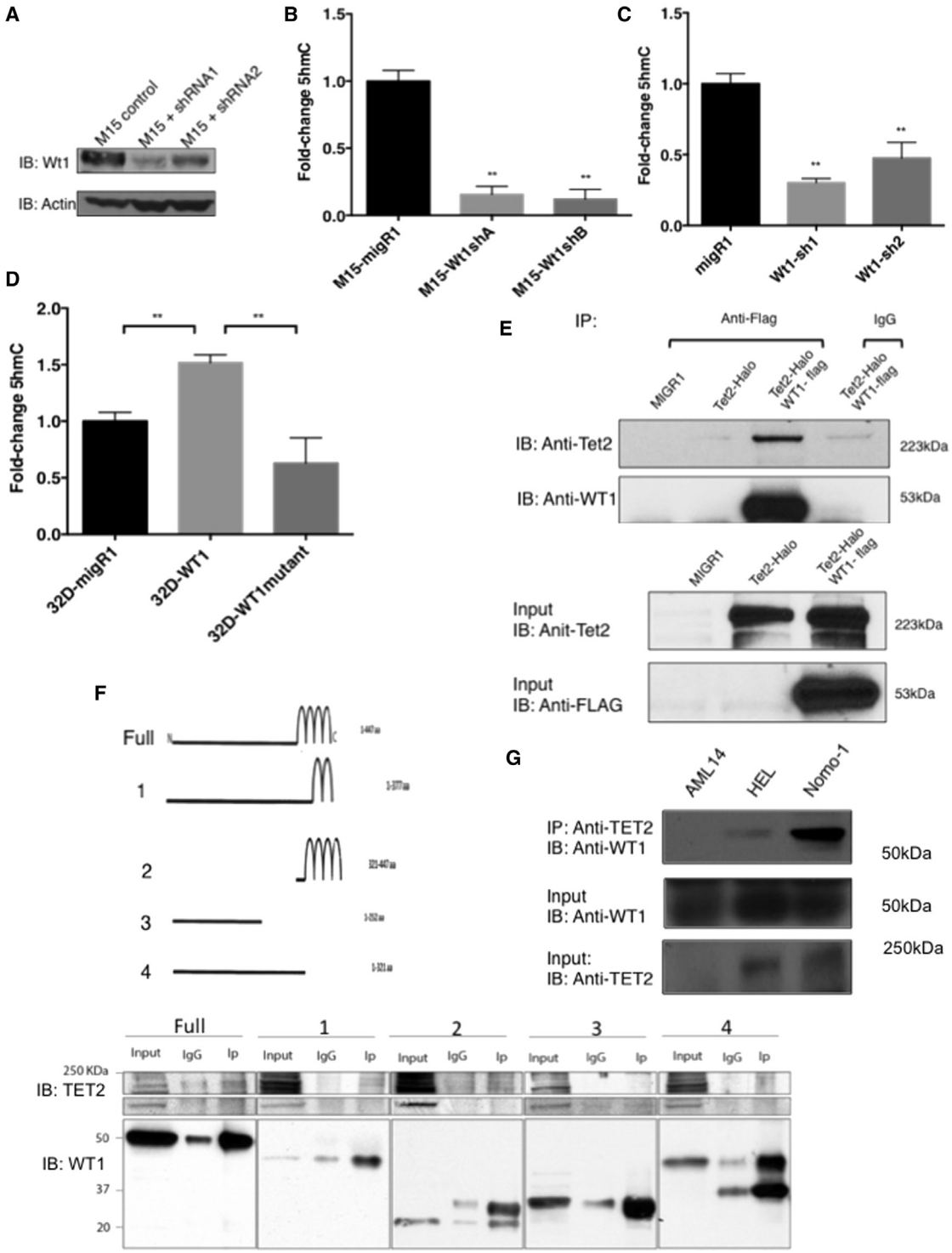


**Figure 5. WT1 Complexes with TET2 and Alterations in Wt1 Levels Result in Changes in 5hmC Levels**

(A) Western blot analysis of Wt1 silencing in mouse mesonephron cells (M15 cells) using vector or shRNA targeting Wt1 (all constructs contained a puromycin resistance marker). Analysis was carried out after puromycin selection.

(B) 5hmC levels were measured by LC-MS from samples of Mouse mesonephron cells (M15) transfected with vector or Wt1-targeted shRNA (both with a puromycin resistance marker) following puromycin selection and confirmation of knockdown.

(C) 5hmC levels were measured by LC-MS from samples of murine whole bone marrow transduced with either vector or Wt1-targeted shRNA.

*(legend continued on next page)*

*IDH1*/*IDH2* mutant AML. Given that *IDH* mutations lead to chemical inhibition of all three TET enzymes, it is not surprising that the impact of *IDH* mutations on global and site specific 5hmC modification are more substantial than in cases with mutations that affect a single TET enzyme (i.e., in TET2 mutant AML) or which impact TET2/TET3 but not TET1 (WT1). Consistent with the convergent mechanism of 5hmC loss, the majority of the loci with altered 5hmC in AMLs with *WT1* and *TET2* mutations represent a subset of the loci with differential 5hmC seen in patients with *IDH1*/*IDH2* mutations. Subsequent functional studies are needed to determine if the "core" set of loci with altered 5hmC are universally altered in all AML patients with *IDH1*/*IDH2*, *WT1*, and *TET2* mutations and how they precisely contribute to leukemic transformation.

In the majority of AML patients, WT1 is not mutated and in fact is overexpressed. WT1 overexpression has been shown to contribute to leukemogenesis (Hosen et al., 2007). As such, WT1 can function as an oncogene and tumor suppressor in AML. WT1 has previously been demonstrated to interact with several different proteins, including p53 (Zhan et al., 1998). Furthermore, through protein-protein interactions, WT1 can suppress the activity of the TCF transcription factor and Wnt pathway targets (Kim et al., 2009). However, the role of these specific functionalities in WT1-mediated hematopoietic transformation is not known. Here, we demonstrate a direct role for WT1 in regulating 5hmC placement in hematopoietic cells through interaction with TET2 and TET3. WT1 loss led to marked reductions in 5hmC levels and a defect in hematopoietic differentiation, a phenotype similar to that observed with loss of TET2. Taken together, these results suggest that the hydroxymethylation pathway may be affected by mutations not previously implicated in epigenetic regulation. We hypothesize there are additional disease alleles that induce transformation through perturbations in TET enzyme function in different malignant contexts.

## EXPERIMENTAL PROCEDURES

### Patient Samples

Three hundred ninety-eight AML samples were obtained at diagnosis from patients enrolled in the E1900 clinical trial (Fernandez et al., 2009). DNA methylation microarrays using the HELP assay was available for 383/398 cases studied for mutational profiling, and gene expression data were available for 325/398 cases. Institutional review board approval was obtained at Weill Cornell Medical College and at Memorial Sloan-Kettering Cancer Center. Eleven human $CD34^+$ bone marrow samples were provided by the Stem Cell and Xenograft Core Facility of the University of Pennsylvania or purchased from AllCells. These studies were performed in accordance with the Helsinki protocols, and all patients provided informed consent.

### Statistical Analysis

Statistical analysis of mutational frequencies was performed using Fisher's exact test. Statistical analysis of colony-forming assays, gene expression levels, c-Kit expression, and 5hmC levels assessed by LC/MS was performed using two-sided t test.

### Constructs

Human WT1 isoform (both containing and not containing a 17 amino acid region within exon 5 as well as the KTS region of the c-terminal) cDNA was cloned into Migr1 (Addgene). WT1 mutant (containing a 17 amino acid region within exon 5) cDNA was cloned into Migr1. TET2 cDNA was subcloned into pCMV6-ENTRY (Origene) with a C-terminal FLAG tag and myc tag. TET1 and TET3 cDNA was synthesized and subcloned into HaloTag vector pFN21A (Promega).

### Cell Culture and Transfection

GP2-293T cells were cultured as previously described (Marubayashi et al., 2010). Transfection was performed with X-treme 9 transfection reagent (Roche). 32D cells were cultured in RPMI-1640 medium (Invitrogen) supplemented with 10% fetal bovine serum and 1 ng/ml recombinant IL-3 (BD Biosciences, 554579).

### Liquid Chromatography-Electron Spray Ionization-Tandem Mass Spectrometry

DNA hydrolysis and LC-MS analysis of 5-methylcytosine and 5-hydroxymethylcytosine was performed as described previously (Vasanthakumar et al., 2013). Please see the Supplemental Experimental Procedures for description of protocol used.

### shRNA Knockdown

*TET2* shRNA was produced as previously described (Figueroa et al., 2010a). WT1 shRNA was produced using previously described and validated target sequence (Vicent et al., 2010) and inserted into a pSIREN vector (Clontech). Wt1 ShRNA in a pLKO-Puromycin vector was generated by the Broad Institute RNAi Consortium. shRNAs (21 nt) targeting mouse Tet3 were designed and cloned into the LMP retroviral vector (Dow et al., 2012). ShRNA sequences are provided in the Supplemental Experimental Procedures. All shRNA experiments were carried out using three biologic replicates and three technical replicates for each condition.

### Western Blot and Coimmunoprecipitation

Cell lysis, immunoprecipitation, and western blot analysis was performed as previously described (Marubayashi et al., 2010). Cell lysis and immunoprecipitation was carried out in buffer containing 150 mM NaCl, 20 mM Tris, 5 mM EDTA, 1% Triton X-100, and 10% glycerol (with addition of protease arrest, phosphatase inhibitor cocktail II, 1 mM phenylmethylsulfonyl fluoride, and 0.02 mM phenylarsine oxide in PBS). Washes were carried out in either PBS or lysis buffer. Anti-FLAG antibodies were purchased from Sigma-Aldrich (F1804) and Novus Biologicals (NBP1-06712). Anti-TET2 antibody was generated as described below. Anti-actin antibody utilized was purchased from Calbiochem (CP01). Anti-WT1 antibodies used for western blot were purchased from Upstate (05-753) and Abcam (ab28428). Anti-TET1 (GTX124207) and anti-TET3 (GTX121453) antibodies were purchased from GeneTex.

### Flow Cytometry

Flow cytometry studies were performed as previously described (Figueroa et al., 2010a). c-Kit coupled to APC (BD Pharmingen) was utilized for c-KIT staining. 5hmC staining, reagents utilized, and analysis were performed as described (Figueroa et al., 2010a). Staining with cleaved caspase-3 was used for apoptosis studies. Staining with DAPI was used for cell-cycle analysis.

(D) 5hmC levels were measured by LC-MS from samples of 32D cells transduced with WT1 isoform D or a WT1 truncation mutant (**$p < 0.01$, t test). No statistically significant difference was observed between 32D cells transduced with migR1 and 32D cells transduced with WT1 mutant. Error bars represent SEM
(E) IP was carried out with anti-FLAG antibody on lysate from GP2/293T-overexpressing vector, TET2-Halo, or both WT1-FLAG isoform D and TET2-Halo. IP was also carried out with an equal amount of rat immunoglobulin G (IgG) on lysate from GP2/293T cells overexpressing both WT1-FLAG and TET2-Halo.
(F) IP performed on lysate from GP2/293T cells overexpressing both full-length or truncated forms of WT1-HA and TET2-Halo. Control IP performed with rat IgG.
(G) IP performed on lysate of Human leukemia cell lines using an anti-TET2 antibody. IP, immunoprecipitation; IB, immunoblot.

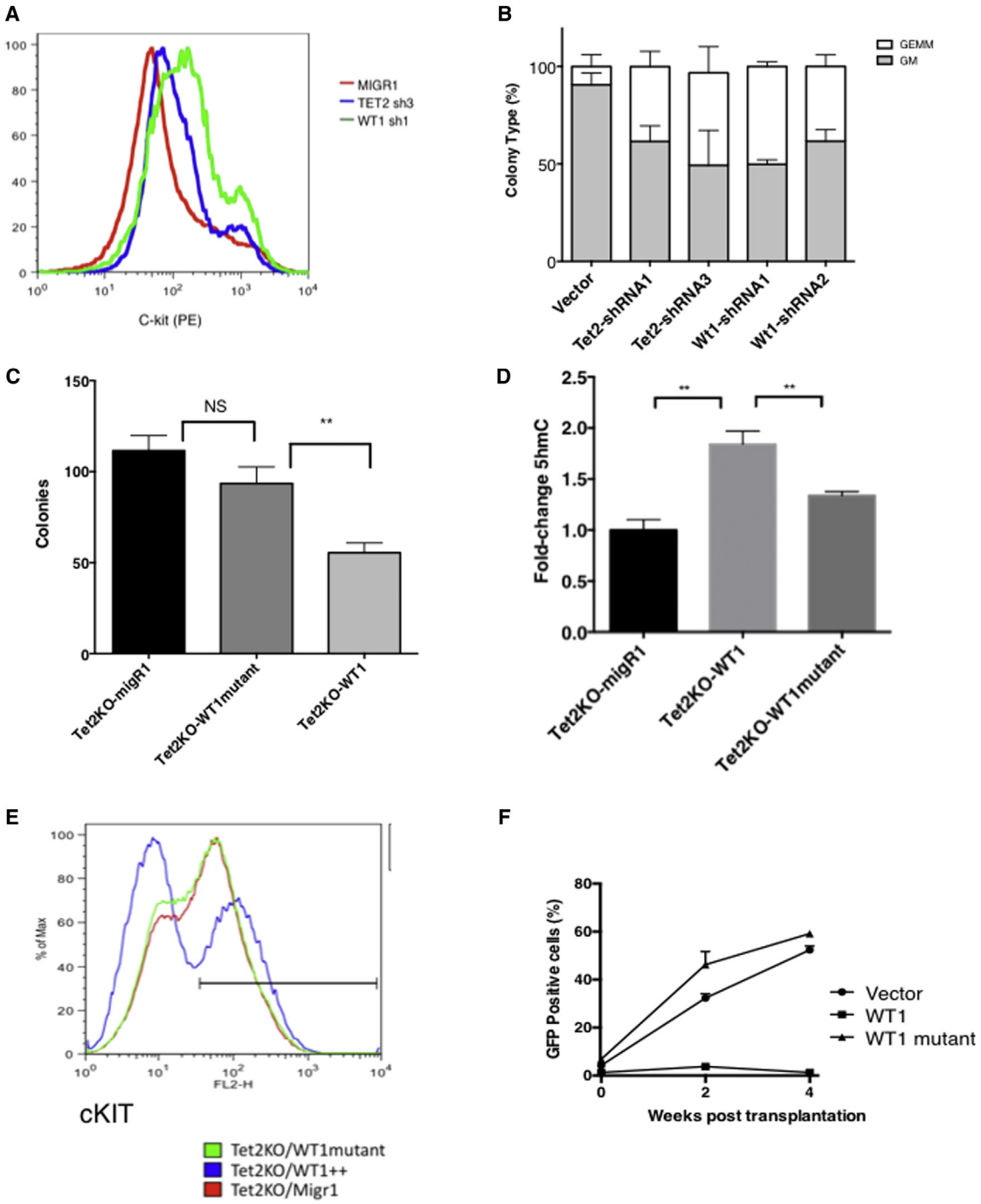


**Figure 6. *Wt1* Silencing Phenocopies *Tet2* Silencing**

(A) Murine bone marrow was transduced with a vector or with shRNA (all constructs containing IRES-GFP) targeting Tet2 or Wt1. GFP-positive cells were selected by flow cytometry. GFP-positive cells were maintained in liquid culture and analyzed by flow for c-KIT expression.

(B) GFP-positive cells were plated in methylcellulose and assessed for colony morphology.

(C) Whole bone marrow extracted from a Tet2 knockout mouse was transduced with vector, WT1 isoform D, or a WT1 truncation mutant GFP-positive cells were selected by flow cytometry. Cells were plated in methylcellulose and colony formation was assessed (**$p < 0.01$ t test).

(D) Cells derived from first methylcellouse plating were analyzed for 5hmC levels by LC-MS (**$p < 0.05$ t test).

(E) GFP-positive cells from initial transduction were also maintained in liquid culture for 3 days and analyzed for c-KIT expression.

(F) Whole bone marrow from Tet2KO mice was transduced with vector, WT1 isoform D, or WT1 mutant. Cells were then injected into lethally irradiated wild-type recipient mice. GFP percentage was assessed from peripheral blood of mice at time points indicated. Error bars represent SEM.

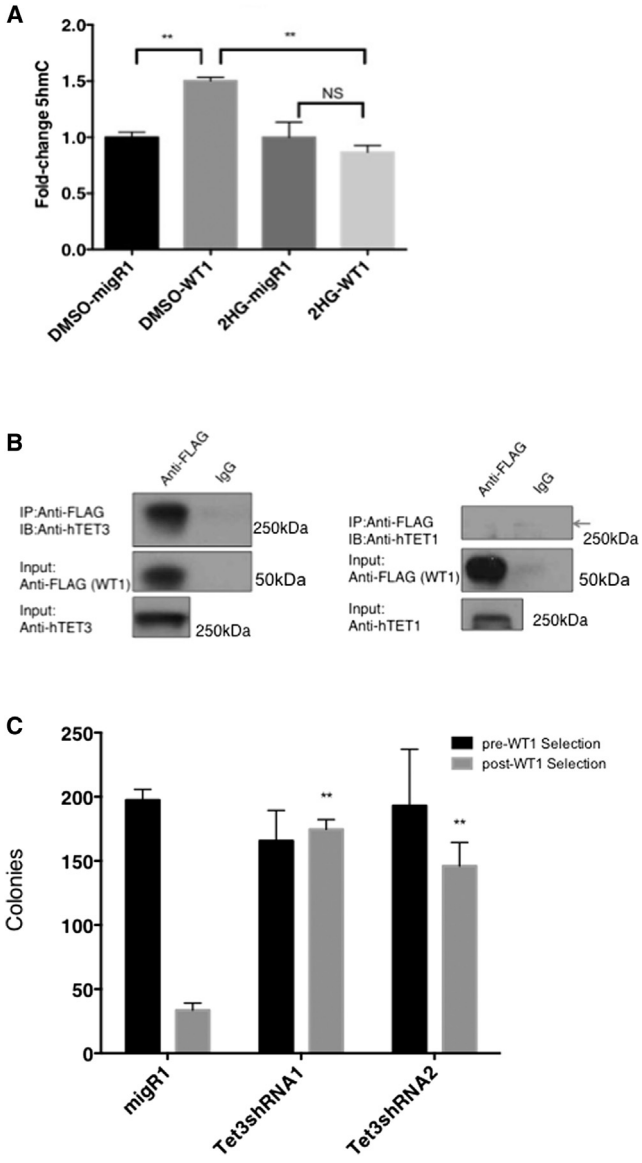


**Figure 7. WT1 Binds to TET3**

(A) GP2/293T cells were transfected with vector or WT1 isoform D. Cells were grown in the presence of DMSO or 2HG. 5hmC levels were subsequently analyzed by LC-MS.

(B) GP2/293T cells were transfected with a WT1-FLAG construct along with TET3 or TET1 construct. IP was carried out with either an anti-FLAG antibody or an equivalent amount of rat IgG.

(C) *Tet2*-deficient BM cells were transduced with empty vector or two different shRNAs targeting *Tet3* (all with IRES GFP). GFP positive cells were sorted for and then transduced with a WT1 construct (with puromycin resistance marker), followed by puromycin selection. Cells were plated in methycellulose, and colonies were counted. Comparison of post-WT1 selection samples demonstrated statistically significant increase in colonies in cells transduced with Tet3 shRNA (**$p < 0.01$). Error bars represent SEM.

### Murine In Vitro Assays

Methylcellulose assays were carried out as previously described (Figueroa et al., 2010a). Animal care was in strict compliance with Memorial Sloan-Kettering Cancer Center, the National Academy of Sciences Guide for the Care and Use of Laboratory Animals, and the Association for Assessment and Accreditation of Laboratory Animal Care guidelines. All methylcellulose assays were carried out with three biologic replicates and four technical replicates per condition.

### Gas Chromatography-Mass Spectrometry

Intracellular 2HG metabolite levels were assayed by GC-MS as previously described (Lu et al., 2012).

## ACCESSION NUMBERS

All ERRBS and hme-Seal data have been deposited to the NCBI Gene Expression Omnibusb under the accession numbers GSE52945 and GSE37454.

## SUPPLEMENTAL INFORMATION

Supplemental Information includes Supplemental Experimental Procedures, seven figures, and four tables and can be found with this article online at http://dx.doi.org/10.1016/j.celrep.2014.11.004.

## AUTHOR CONTRIBUTIONS

R.R., A.A., C.E.M., L.A.G., A.M., M.E.F., and R.L.L. designed the study. R.R., A.A., J.M., A.V., E.P., J.A., O.A.-W., Y.L., C.L., P.S.W., J.J.T., and J.E.T. performed the experiments. Y.L., A.S., V.T., D.D., L.C., and F.F. generated reagents used in experiments. X.Z., Q.D., and C.H. assisted with LC-MS and dot-blot assays. R.R., A.A., J.P., T.H., I.A., M.S.T., A.F., S.N., E.P., C.B.T., J.D.L., C.E.M., L.A.G., A.M., M.E.F., and R.L.L. analyzed the data. R.R., A.A., C.E.M., L.A.G., A.M., M.E.F., and R.L.L. prepared the manuscript with input from the other authors.

## ACKNOWLEDGMENTS

This work was supported by a grant from the National Cancer Institute Physical Sciences Oncology Center (U54CA143798-01) to R.L.L., A.M., and J.D.L., a Leukemia and Lymphoma Society Specialized Center of Research (LLS SCOR) grant to S.D.N., an LLS SCOR to J.D.L. and A.M., a grant from the Gabrielle's Angel Fund to R.L.L., C.H., and A.M.M., grant CA172636-01 to R.L.L., I.A., and A.M., and grants CA129831 and CA129831-03S1 to L.A.G. A.V. is supported by an NIH F32 award. C.E.M. and A.A. are supported by R01HG006798, R01NS076465. M.E.F. is supported by a Leukemia and Lymphoma Society Special Fellow award and a Doris Duke Charitable Foundation Clinical Scientist Development award. O.A.-W. is an American Society of Hematology Basic Research Fellow. A.M. is a Burroughs Wellcome Clinical Translational Scholar. A.M. also is also supported by the Sackler Center for Biomedical and Physical Sciences. R.L.L. and A.F. are funded by Leukemia and Lymphoma Society Scholar Awards. R.R. is an American Society of Hematology Basic Research Fellow. We thank Vicki Huff for kindly providing WT1 truncation constructs.

Received: August 15, 2014
Revised: October 4, 2014
Accepted: November 4, 2014
Published: December 4, 2014

## REFERENCES

Abbas, S., Erpelinck-Verschueren, C.A.J., Goudswaard, C.S., Löwenberg, B., and Valk, P.J.M. (2010). Mutant Wilms' tumor 1 (WT1) mRNA with premature termination codons in acute myeloid leukemia (AML) is sensitive to nonsense-mediated RNA decay (NMD). Leukemia *24*, 660–663.

Bell, J.T., Pai, A.A., Pickrell, J.K., Gaffney, D.J., Pique-Regi, R., Degner, J.F., Gilad, Y., and Pritchard, J.K. (2011). DNA methylation patterns associate with genetic and gene expression variation in HapMap cell lines. Genome Biol. *12*, R10.

Bernt, K.M., Zhu, N., Sinha, A.U., Vempati, S., Faber, J., Krivtsov, A.V., Feng, Z., Punt, N., Daigle, A., Bullinger, L., et al. (2011). MLL-rearranged leukemia is dependent on aberrant H3K79 methylation by DOT1L. Cancer Cell *20*, 66–78.

Bullinger, L., Ehrich, M., Döhner, K., Schlenk, R.F., Döhner, H., Nelson, M.R., and van den Boom, D. (2010). Quantitative DNA methylation predicts survival in adult acute myeloid leukemia. Blood *115*, 636–642.

Daigle, S.R., Olhava, E.J., Therkelsen, C.A., Majer, C.R., Sneeringer, C.J., Song, J., Johnston, L.D., Scott, M.P., Smith, J.J., Xiao, Y., et al. (2011). Selective killing of mixed lineage leukemia cells by a potent small-molecule DOT1L inhibitor. Cancer Cell *20*, 53–65.

Dawson, M.A., Prinjha, R.K., Dittmann, A., Giotopoulos, G., Bantscheff, M., Chan, W.I., Robson, S.C., Chung, C.W., Hopf, C., Savitski, M.M., et al. (2011). Inhibition of BET recruitment to chromatin as an effective treatment for MLL-fusion leukaemia. Nature *478*, 529–533.

Dow, L.E., Premsrirut, P.K., Zuber, J., Fellmann, C., McJunkin, K., Miething, C., Park, Y., Dickins, R.A., Hannon, G.J., and Lowe, S.W. (2012). A pipeline for the generation of shRNA transgenic mice. Nat. Protoc. *7*, 374–393.

Ernst, T., Chase, A.J., Score, J., Hidalgo-Curtis, C.E., Bryant, C., Jones, A.V., Waghorn, K., Zoi, K., Ross, F.M., Reiter, A., et al. (2010). Inactivating mutations of the histone methyltransferase gene EZH2 in myeloid disorders. Nat. Genet. *42*, 722–726.

Fernandez, H.F., Sun, Z., Yao, X., Litzow, M.R., Luger, S.M., Paietta, E.M., Racevskis, J., Dewald, G.W., Ketterling, R.P., Bennett, J.M., et al. (2009). Anthracycline dose intensification in acute myeloid leukemia. N. Engl. J. Med. *361*, 1249–1259.

Figueroa, M.E., Abdel-Wahab, O., Lu, C., Ward, P.S., Patel, J., Shih, A., Li, Y., Bhagwat, N., Vasanthakumar, A., Fernandez, H.F., et al. (2010a). Leukemic IDH1 and IDH2 mutations result in a hypermethylation phenotype, disrupt TET2 function, and impair hematopoietic differentiation. Cancer Cell *18*, 553–567.

Figueroa, M.E., Lugthart, S., Li, Y., Erpelinck-Verschueren, C., Deng, X., Christos, P.J., Schifano, E., Booth, J., van Putten, W., Skrabanek, L., et al. (2010b). DNA methylation signatures identify biologically distinct subtypes in acute myeloid leukemia. Cancer Cell *17*, 13–27.

Filippakopoulos, P., Qi, J., Picaud, S., Shen, Y., Smith, W.B., Fedorov, O., Morse, E.M., Keates, T., Hickman, T.T., Felletar, I., et al. (2010). Selective inhibition of BET bromodomains. Nature *468*, 1067–1073.

Giannopoulou, E.G., and Elemento, O. (2011). An integrated ChIP-seq analysis platform with customizable workflows. BMC Bioinformatics *12*, 277.

Haber, D.A., Sohn, R.L., Buckler, A.J., Pelletier, J., Call, K.M., and Housman, D.E. (1991). Alternative splicing and genomic structure of the Wilms tumor gene WT1. Proc. Natl. Acad. Sci. USA *88*, 9618–9622.

Hosen, N., Shirakata, T., Nishida, S., Yanagihara, M., Tsuboi, A., Kawakami, M., Oji, Y., Oka, Y., Okabe, M., Tan, B., et al. (2007). The Wilms' tumor gene WT1-GFP knock-in mouse reveals the dynamic regulation of WT1 expression in normal and leukemic hematopoiesis. Leukemia *21*, 1783–1791.

Kim, M.K., Mason, J.M., Li, C.M., Berkofsky-Fessler, W., Jiang, L., Choubey, D., Grundy, P.E., Tycko, B., and Licht, J.D. (2008). A pathologic link between Wilms tumor suppressor gene, WT1, and IFI16. Neoplasia *10*, 69–78.

Kim, M.K., McGarry, T.J., O Broin, P., Flatow, J.M., Golden, A.A., and Licht, J.D. (2009). An integrated genome screen identifies the Wnt signaling pathway as a major target of WT1. Proc. Natl. Acad. Sci. USA *106*, 11154–11159.

Ko, M., Huang, Y., Jankowska, A.M., Pape, U.J., Tahiliani, M., Bandukwala, H.S., An, J., Lamperti, E.D., Koh, K.P., Ganetzky, R., et al. (2010). Impaired hydroxylation of 5-methylcytosine in myeloid cancers with mutant TET2. Nature *468*, 839–843.

Konstandin, N., Bultmann, S., Szwagierczak, A., Dufour, A., Ksienzyk, B., Schneider, F., Herold, T., Mulaw, M., Kakadia, P.M., Schneider, S., et al. (2011). Genomic 5-hydroxymethylcytosine levels correlate with TET2 mutations and a distinct global gene expression pattern in secondary acute myeloid leukemia. Leukemia *25*, 1649–1652.

Kulis, M., Heath, S., Bibikova, M., Queirós, A.C., Navarro, A., Clot, G., Martínez-Trillos, A., Castellano, G., Brun-Heath, I., Pinyol, M., et al. (2012). Epigenomic analysis detects widespread gene-body DNA hypomethylation in chronic lymphocytic leukemia. Nat. Genet. *44*, 1236–1242.

Larsson, S.H., Charlieu, J.P., Miyagawa, K., Engelkamp, D., Rassoulzadegan, M., Ross, A., Cuzin, F., van Heyningen, V., and Hastie, N.D. (1995). Subnuclear localization of WT1 in splicing or transcription factor domains is regulated by alternative splicing. Cell *81*, 391–401.

Ley, T.J., Ding, L., Walter, M.J., McLellan, M.D., Lamprecht, T., Larson, D.E., Kandoth, C., Payton, J.E., Baty, J., Welch, J., et al. (2010). DNMT3A mutations in acute myeloid leukemia. N. Engl. J. Med. *363*, 2424–2433.

Li, Z., Cai, X., Cai, C.L., Wang, J., Zhang, W., Petersen, B.E., Yang, F.C., and Xu, M. (2011). Deletion of Tet2 in mice leads to dysregulated hematopoietic stem cells and subsequent development of myeloid malignancies. Blood *118*, 4509–4518.

Lian, C.G., Xu, Y., Ceol, C., Wu, F., Larson, A., Dresser, K., Xu, W., Tan, L., Hu, Y., Zhan, Q., et al. (2012). Loss of 5-hydroxymethylcytosine is an epigenetic hallmark of melanoma. Cell *150*, 1135–1146.

Lu, C., Ward, P.S., Kapoor, G.S., Rohle, D., Turcan, S., Abdel-Wahab, O., Edwards, C.R., Khanin, R., Figueroa, M.E., Melnick, A., et al. (2012). IDH mutation impairs histone demethylation and results in a block to cell differentiation. Nature *483*, 474–478.

Marubayashi, S., Koppikar, P., Taldone, T., Abdel-Wahab, O., West, N., Bhagwat, N., Caldas-Lopes, E., Ross, K.N., Gönen, M., Gozman, A., et al. (2010). HSP90 is a therapeutic target in JAK2-dependent myeloproliferative neoplasms in mice and humans. J. Clin. Invest. *120*, 3578–3593.

Moran-Crusio, K., Reavie, L., Shih, A., Abdel-Wahab, O., Ndiaye-Lobry, D., Lobry, C., Figueroa, M.E., Vasanthakumar, A., Patel, J., Zhao, X., et al. (2011). Tet2 loss leads to increased hematopoietic stem cell self-renewal and myeloid transformation. Cancer Cell *20*, 11–24.

Nishida, S., Hosen, N., Shirakata, T., Kanato, K., Yanagihara, M., Nakatsuka, S., Hoshida, Y., Nakazawa, T., Harada, Y., Tatsumi, N., et al. (2006). AML1-ETO rapidly induces acute myeloblastic leukemia in cooperation with the Wilms tumor gene, WT1. Blood *107*, 3303–3312.

Oji, Y., Miyoshi, S., Maeda, H., Hayashi, S., Tamaki, H., Nakatsuka, S., Yao, M., Takahashi, E., Nakano, Y., Hirabayashi, H., et al. (2002). Overexpression of the Wilms' tumor gene WT1 in de novo lung cancers. Int. J. Cancer *100*, 297–303.

Patel, J.P., Gönen, M., Figueroa, M.E., Fernandez, H., Sun, Z., Racevskis, J., Van Vlierberghe, P., Dolgalev, I., Thomas, S., Aminova, O., et al. (2012). Prognostic relevance of integrated genetic profiling in acute myeloid leukemia. N. Engl. J. Med. *366*, 1079–1089.

Quivoron, C., Couronné, L., Della Valle, V., Lopez, C.K., Plo, I., Wagner-Ballon, O., Do Cruzeiro, M., Delhommeau, F., Arnulf, B., Stern, M.H., et al. (2011). TET2 inactivation results in pleiotropic hematopoietic abnormalities in mouse and is a recurrent event during human lymphomagenesis. Cancer Cell *20*, 25–38.

Song, C.X., Szulwach, K.E., Fu, Y., Dai, Q., Yi, C., Li, X., Li, Y., Chen, C.H., Zhang, W., Jian, X., et al. (2011). Selective chemical labeling reveals the genome-wide distribution of 5-hydroxymethylcytosine. Nat. Biotechnol. *29*, 68–72.

Stroud, H., Feng, S., Morey Kinney, S., Pradhan, S., and Jacobsen, S.E. (2011). 5-Hydroxymethylcytosine is associated with enhancers and gene bodies in human embryonic stem cells. Genome Biol. *12*, R54.

Vasanthakumar, A., Lepore, J.B., Zegarek, M.H., Kocherginsky, M., Singh, M., Davis, E.M., Link, P.A., Anastasi, J., Le Beau, M.M., Karpf, A.R., and Godley, L.A. (2013). Dnmt3b is a haploinsufficient tumor suppressor gene in Myc-induced lymphomagenesis. Blood *121*, 2059–2063.

Vicent, S., Chen, R., Sayles, L.C., Lin, C., Walker, R.G., Gillespie, A.K., Subramanian, A., Hinkle, G., Yang, X., Saif, S., et al. (2010). Wilms tumor 1 (WT1) regulates KRAS-driven oncogenesis and senescence in mouse and human models. J. Clin. Invest. *120*, 3940–3952.

Wang, Z.Y., Qiu, Q.Q., Enger, K.T., and Deuel, T.F. (1993). A second transcriptionally active DNA-binding site for the Wilms tumor gene product, WT1. Proc. Natl. Acad. Sci. USA *90*, 8896–8900.

Wang, G.G., Song, J., Wang, Z., Dormann, H.L., Casadio, F., Li, H., Luo, J.L., Patel, D.J., and Allis, C.D. (2009). Haematopoietic malignancies caused by dysregulation of a chromatin-binding PHD finger. Nature *459*, 847–851.

Xu, W., Yang, H., Liu, Y., Yang, Y., Wang, P., Kim, S.H., Ito, S., Yang, C., Wang, P., Xiao, M.T., et al. (2011). Oncometabolite 2-hydroxyglutarate is a competitive inhibitor of α-ketoglutarate-dependent dioxygenases. Cancer Cell *19*, 17–30.

Yan, X.J., Xu, J., Gu, Z.H., Pan, C.M., Lu, G., Shen, Y., Shi, J.Y., Zhu, Y.M., Tang, L., Zhang, X.W., et al. (2011). Exome sequencing identifies somatic mutations of DNA methyltransferase gene DNMT3A in acute monocytic leukemia. Nat. Genet. *43*, 309–315.

Yu, M., Hon, G.C., Szulwach, K.E., Song, C.X., Zhang, L., Kim, A., Li, X., Dai, Q., Shen, Y., Park, B., et al. (2012). Base-resolution analysis of 5-hydroxymethylcytosine in the mammalian genome. Cell *149*, 1368–1380.

Zhan, Q., Chen, I.T., Antinore, M.J., and Fornace, A.J., Jr. (1998). Tumor suppressor p53 can participate in transcriptional induction of the GADD45 promoter in the absence of direct DNA binding. Mol. Cell. Biol. *18*, 2768–2778.

Zuber, J., Shi, J., Wang, E., Rappaport, A.R., Herrmann, H., Sison, E.A., Magoon, D., Qi, J., Blatt, K., Wunderlich, M., et al. (2011). RNAi screen identifies Brd4 as a therapeutic target in acute myeloid leukaemia. Nature *478*, 524–528.